

Privacy-Aware Spectrum Pricing and Power Control Optimization for LEO Satellite Internet-of-Things

Bowen Shen, Kwok-Yan Lam, *Senior Member, IEEE* and Feng Li, *Member, IEEE*

Abstract—Low earth orbit (LEO) satellite systems play an important role in next generation communication networks due to their ability to provide extensive global coverage with guaranteed communications in remote areas and isolated areas where base stations cannot be cost-efficiently deployed. With the pervasive adoption of LEO satellite systems, especially in the LEO Internet-of-Things (IoT) scenarios, their spectrum resource management requirements have become more complex as a result of massive service requests and high bandwidth demand from terrestrial terminals. For instance, when leasing the spectrum to terrestrial users and controlling the uplink transmit power, satellites collect user data for machine learning purposes, which usually are sensitive information such as location, budget and quality of service (QoS) requirement. To facilitate model training in LEO IoT while preserving the privacy of data, blockchain-driven federated learning (FL) is widely used by leveraging on a fully decentralized architecture. In this paper, we propose a hybrid spectrum pricing and power control framework for LEO IoT by combining blockchain technology and FL. We first design a local deep reinforcement learning algorithm for LEO satellite systems to learn a revenue-maximizing pricing and power control scheme. Then the agents collaborate to form a FL system. We also propose a reputation-based blockchain which is used in the global model aggregation phase of FL. Based on the reputation mechanism, a node is selected for each global training round to perform model aggregation and block generation, which can further enhance the decentralization of the network and guarantee the trust. Simulation tests are conducted to evaluate the performances of the proposed scheme. Our results show the efficiency of finding the maximum revenue scheme for LEO satellite systems while preserving the privacy of each agent. Lastly, we also compare several FL aggregation algorithms to better illustrate the performances of the scheme.

Index Terms—Satellite communications, spectrum allocation, federated learning, blockchain

I. INTRODUCTION

FOR many regions such as oceans and deserts, which account for most of the earth's surface, it is not easy to deploy massive base stations (BSs) to support continuously upgrading wireless demands and massive Internet-of-Things (IoT) terminals [1], [2]. As the extension of terrestrial BSs, satellite communications especially low earth orbit (LEO) satellite communications have attracted many researchers' and practitioners' interest due to the advantage of highly global coverage and guaranteed communications [3]. Many satellite operators such as Starlink, OneWeb, Amazon and Boeing have

launched or are planning to launch LEO satellite networks to cover millions of potential terrestrial terminals [4]–[6]. The low orbital altitude of the satellite makes the transmission delay shorter and the path loss smaller compared to geostationary earth orbit (GEO) satellites, and the constellation composed of multiple satellites can achieve global coverage. Besides, cellular communication, multiple access, point beam, frequency multiplexing and other technologies also provide the technical guarantee for LEO satellite communications. Sixth generation (6G) communications, which are built on the base of LEO satellite networks, will be driven by the surging artificial intelligence (AI), big data, and Internet of Everything (IoE) technologies. In this context, the mobile networks of 6G and beyond are expected to not only enhance the key performance indicators and quality of service (QoS) of 5G continuously but also introduce numerous novel technologies and use cases [7].

With the blooming terrestrial IoT applications in recent years, existing wireless resources can not meet the requirements in many fields including vehicular communications, industrial automation, sensor networks, and public safety [8]–[11]. As the demand for spectrum resources and the number of massive user access increases rapidly, how to manage spectrum resources efficiently has become a key challenge for LEO satellite communication networks [12]. Many techniques including dynamic spectrum access (DSA), non-orthogonal multiple access (NOMA), cognitive radio (CR) and multiple spot beams have been proposed to alleviate the pressure on spectrum resource usage [13]–[16]. In most scenarios when using DSA, deep learning is applied to train a model for resource allocation [17]. Hence, satellites need to guarantee computing power for the model training. In [18], the authors combined the NOMA and orthogonal frequency division multiplexing to improve spectrum efficiency. In the utilization of cognitive radio (CR), wireless communication systems adaptively adjust their transmitting parameters by sensing the current communication environment. This adaptive approach enables efficient utilization of spectrum resources [16]. The multiple spot beams technique can transfer a wide beam into multiple beams to increase the coverage gain of a satellite antenna, wherein interference between beams will affect the performance of the system [19].

In recent years, self-learning-based methods, especially deep reinforcement learning (DRL) have become a focus in the field of DSA and spectrum sensing [20]–[22]. Each user has a model that is regarded as Agent that continually updates its parameters during training. The Agent interacts with the communication environment to find the optimal scheme. In order to

B. Shen and K. Lam are with School of Computer Science and Engineering, Nanyang Technological University, 639798, Singapore. (bowen010@e.ntu.edu.sg, kwokyan.lam@ntu.edu.sg) F. Li is with Strategic Centre for Research in Privacy-Preserving Technologies and Systems, Nanyang Technological University, 639798, Singapore. (li_feng@ntu.edu.sg)

enhance the cooperation among satellite nodes during training and to improve the training efficiency while still preserving the privacy of each node, federated learning (FL) and blockchain technology attract much attention [23]–[25]. In the FL training process, each node’s local model parameters instead of raw data are uploaded to the blockchain network. Then, a node is selected by the blockchain generation mechanism to conduct global model aggregation for the global training round. Such FL-based schemes improve the training efficiency of each node and also enhance the decentralization degree of the distributed system.

In this paper, based on blockchain-driven FL, we introduce a privacy-aware spectrum pricing and uplink transmit power control optimization scheme for LEO satellite IoT. Specifically, we first formulate the price bargaining and power control between terrestrial users and LEO satellites as a Markov decision process. The service quality requirements of each terrestrial user and the condition of the satellites’ spectrum change frequently. Deployment of reinforcement learning allows pricing and power control schemes to be adjusted in real time based on the changing environment. We use the Double Deep Q-learning to train a neural network model for each LEO satellite to find the optimal spectrum price and power control level. Besides, due to the limited battery capacity of LEO satellites, it is impractical to consume large amounts of power for model training on satellites. Thus, each LEO satellite has a terrestrial server for data computing. After receiving information from terrestrial users, the LEO satellite then sends it to the corresponding terrestrial server for model training. Considering different nodes have different computation power and the transaction information needs to be kept highly confidential, FL is applied in this paper for satellites’ model training collaboration while privacy preservation is guaranteed to some degree. Traditional FL usually has a central server for global model aggregation and release. Thus, each node needs to give quite a lot of trust to the central server and the whole system will be paralyzed if the central server is malicious. To enhance the decentralization of the LEO satellite IoT networks, we introduce blockchain technology in the global model aggregation phase of FL. A reputation-based consensus mechanism is proposed based on the feature of transactions between terrestrial users and LEO satellites. Each LEO satellite that participates in the FL has a reputation record that determines the node to conduct the model aggregation and block generation in the global training round. And the behaviors of users who trade with the satellite will be used as the basis for increasing or decreasing the satellite’s reputation.

The contributions of this paper can be highlighted as follows.

- A reinforcement learning problem is formulated based on the Markov decision process to obtain an optimal policy for maximizing the benefits of LEO satellite systems by optimizing spectrum pricing and power control.
- A DRL-based spectrum pricing and power control scheme is proposed for LEO satellite IoT. We take into account the interference among terrestrial users in the same cell and try to find the optimal spectrum and

TABLE I
SUMMARY OF SYMBOLS AND NOTATIONS

Symbols	Notations
d_o^s	Distance between satellite and cell center
d_{Mn}^s	Distance between satellite and user (M, n)
R	Earth radius
d_{Mn}^o	Distance between cell center o and user (M, n)
$\mathcal{P}_{n,t}$	Transmit power of satellite terminal
θ_n	Elevation angle from user (M, n) to the satellite system
$g_{n,t}(\theta_n)$	Antenna gain of user (M, n) at the direction θ_n
$\alpha_{n,t}^M$	Derivation angle form user (M, n) to the central line of cell M
$G_{M,t}(\alpha_n^M)$	Satellite antenna gain of cell M at the direction α_n^M
$d_{n,t}$	Straight-line distance between the user (M, n) and the satellite system
λ	wavelength
$f_{n,t}(\theta_n)$	Channel fading of user (M, n) at the direction θ_n
μ_a	Active factor of user a at cell H which is related to the user’s service type
ρ_{H}^M	Polarization isolation factor between cell M and H
σ^2	Power of noise
$p^{m,t}$	Spectrum pricing given by the satellite
$N_{pri,t}^m$	Number of users willing to lease this spectrum at the pricing p_t^m
\hat{p}	Power utilization coefficient
l_t^m	Power control level of the satellite
$N_{pow,t}^m$	Number of users whose transmit power is lower than l_t^m
$u_{f,t}$	Terrestrial users’ utility at time slot t
C^m	Spectrum quality of satellite m
I_t	Average interference level at time slot t
\mathcal{S}	State
\mathcal{A}	Action
\mathcal{R}	Reward
Rep	Reputation token

power management scheme to balance the interference and maximize the benefits of LEO satellites.

- A blockchain-driven FL framework is designed. Based on the transaction characteristic between terrestrial users and LEO satellites, we introduce a reputation-based mechanism to the blockchain network to select nodes for block generation and global model aggregation.
- Simulation tests are conducted to show the performances of the proposed schemes.

The rest of this paper is organized as follows. Section II introduces the system model of the proposed scheme. In section III, we detail the scheme of the DRL-based spectrum pricing and power control. And the framework of blockchain-driven FL is also presented. Section IV shows the numerical results and section V concludes this paper finally.

II. RELATED WORK

Many mathematical tools including Stackelberg game model have been widely explored to optimize spectrum resource utilization in satellite networks [26]–[28]. In [26], the authors designed a multi-leader multi-follower Stackelberg game to achieve spectrum pricing. Seller operators, who are regarded as leaders, determine the pricing strategies based on the buying strategies of buyer operators who are regarded as followers. The authors defined the seller operations’ revenue function as the income by providing bandwidth to buyer operators

minus the service cost and charge for the primary node. And the buyer operations' revenue was expressed as an increasing function of the bought bandwidth. Then a Stackelberg game was formulated based on the two functions. In [27], the author formulated the problem of bandwidth pricing and allocation by employing a Stackelberg game-theoretic approach to model the interactions between spectrum providers and customers. Subsequently, the study analyzed the Stackelberg game equilibrium under two pricing strategies: uniform pricing and differential pricing. In the case of differential pricing, adjustments are made to individual customer prices based on various heterogeneous factors. In [28], game theory was used to model the wireless users' competition over shared spectrum. The author assumed that users who adjust a transmission power level to maximize their own utilities are players. And the utility of a player was evaluated based on the transmission rate.

With the increasing computing power of mobile devices, the deployment of machine learning-based algorithms in satellite resource allocation attracts more attention [29], [30]. Satya Chan *et al.* [29] proposed a low complexity power and frequency resource allocation method to minimize inter-component interference while maximizing user throughput. This work first used a pre-trained perception to classify the condition of the traffic demand and then employed a projection tool to minimize the traffic demand reduction. Finally, a pre-trained linear regression model was introduced to allocate bandwidths. The scheme has excellent performance while keeping the low complexity of the algorithm. In [30], considering terrestrial users' limited battery capacity and each LEO satellite's computation capability, the authors trained a deep neural network model to minimize the total execution delay of terrestrial users.

In most satellite resource allocation scenarios, the complete information and environment conditions are generally difficult to get due to the dynamic environments. Hence, DRL has been adopted to address optimization problems in IoT networks. In [31], [32], the authors introduced the DRL methods in multibeam satellite systems for dynamic resource allocation. And multi-agent DRL scheme was proposed in [32] to better address the cooperative game problems. Recently, there have been some studies about federated DRL (FDRL) for further collaborations between nodes in satellite IoT [33]–[35]. In [33], the authors designed an adaptive FDRL scheme to find efficient task offloading and energy-saving policy considering the scenario of space-air-ground integrated edge computing. Considering the high communication costs and aggregation execution time, an asynchronous FL framework combined with a multi-agent asynchronous advantage actor-critic (A3C)-based joint device selection algorithm was proposed in [34]. The scheme allows the users to update and aggregate the local model parameters asynchronously instead of waiting for devices with low computation powers. Besides, due to the A3C-based algorithm, the federated execution time and learning accuracy loss are effectively minimized.

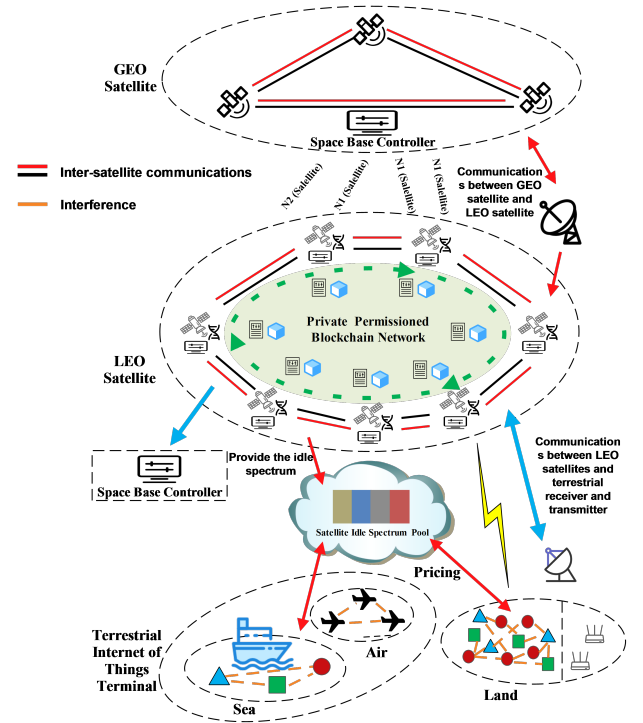


Fig. 1. System model

III. SYSTEM MODEL

A. Satellite Network Architecture

The spectrum pricing and sharing scheme in this paper is based on the LEO satellite IoT whose architecture is illustrated in Fig 1. It is assumed that the satellite payload is equipped with necessary modules such as multi-port amplifiers, flexible traveling wave tube amplifiers, etc. The scenario considered is that IoT nodes of terrestrial users are connected to LEO satellites through terrestrial cluster heads or BS. The terrestrial users carry transceivers compatible with both cellular and satellite data transmissions so that the cluster heads can communicate with the cluster members. LEO satellites share or lease their idle spectrum to terrestrial users directly or with the assistance of the GEO satellites to improve the utilization of the spectrum and increase their revenues. Each satellite has a terrestrial server for data computing and machine learning. Besides, these terrestrial servers are responsible for participating in FL for model training collaboration and a reputation-based blockchain due to the privacy preservation concern. During the process, based on the needs of the cluster members, the cluster head responds as a transaction agent to the spectrum pricing and power control scheme given by the LEO satellite. It is noted that seamless coverage of the terrestrial server by LEO satellite is significant to ensure timely transmission of model parameters. Inter-satellite links are utilized to establish connections both within and between satellite constellations, enabling LEO satellites to relay data. Additionally, some of these satellites are equipped with onboard processing and storage capabilities, facilitating satellite-borne computing.

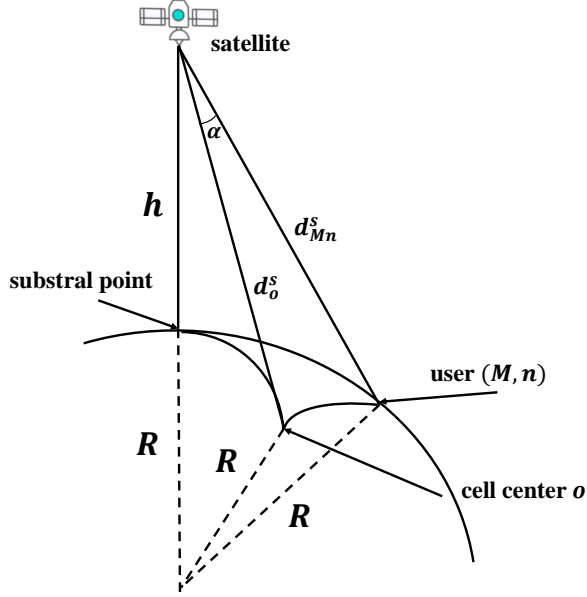


Fig. 2. oblique projector

B. Interference Model

According to the satellite network architecture in this paper, the multi-beam antenna technique is applied. In this case, the Earth's surface is considered as a plane and the satellites project the beam onto the Earth's surface [26]. Unlike the propagation characteristics of high-orbiting satellites, there are more LEO satellites and more low earth orbits, thus LEO satellites fly faster and cover a highly variable area. This makes the situation where most of the LEO satellites' projection cells are not under the mode of orthographic projection even more prominent. Similar to the current existing work [36], this paper considers the effect of the angle between the position of the selected user and the central line of the corresponding beam on the interference intensity. Thus, the angle α describing the deviation angle between user (M, n) and cell center o can be expressed as

$$\alpha = \arccos\left(\frac{(d_o^s)^2 + (d_{Mn}^s)^2 - 2R^2(1 - \cos(d_{Mn}^o/R))}{(2d_o^s d_{Mn}^s)^{-1}}\right) \quad (1)$$

where d_o^s denotes the distance between the satellite and cell center, d_{Mn}^s denotes the distance between satellite and user (M, n) , R denotes the earth radius, d_{Mn}^o denotes the distance between cell center o and user (M, n) as shown in Fig. 2. It is assumed that the idle spectrum of an LEO satellite is first divided into multiple channels by orthogonal frequency-division multiple access (OFDMA). Then each channel is leased to multiple users on the ground by time division multiple access. (TDMA). Inter-cell interference should be considered. For the uplink channel, the receiving power at the satellite at time slot t from user n at cell M can be expressed as

$$P_t = \frac{\mathcal{P}_{n,t} g_{n,t}(\theta_n) G_{M,t}(\alpha_n^M)}{\left(\frac{4\pi d_{n,t}}{\lambda}\right)^2 f_{n,t}(\theta_n)} \quad (2)$$

where $\mathcal{P}_{n,t}$ denotes the transmit power of satellite terminal θ_n denotes the elevation angle from user (M, n) to the satellite system, $g_{n,t}(\theta_n)$ denotes the antenna gain of user (M, n) at the direction θ_n , α_n^M is the derivation angle form user (M, n) to the central line of cell M , $G_{M,t}(\alpha_n^M)$ is the satellite antenna gain of cell M at the direction α_n^M , $d_{n,t}$ is the straight-line distance between the user (M, n) and the satellite system, λ denotes the wavelength, $f_{n,t}(\theta_n)$ denotes the channel fading of user (M, n) at the direction θ_n .

The interference among the terrestrial cells can be given as

$$I_t = \sum_{H=1}^k \frac{\mathcal{P}_{a,t} g_{a,t}(\theta_n) G_{H,t}(\theta_a^H)}{(4\pi d_{a,t}/\lambda)^2 f_{a,t}(\theta_n)} \mu_a \rho_H^M \quad (3)$$

where μ_a denotes the active factor of user a at cell H which is related to the user's service type. ρ_H^M is the polarization isolation factor between cell M and H .

Hence, the uplink Signal to Interference plus Noise Ratio (SINR) can be expressed as

$$SINR_t = \frac{p_{n,t} g_{n,t}(\theta_n) G_{M,t}(\alpha_n^M) c^2}{f_{n,t}(\theta_n) d_{n,t}^2 I_t + \sigma^2} \quad (4)$$

where σ^2 denotes the power of noise.

C. Security Threats

FL is introduced in this paper for machine learning collaborations among LEO satellite nodes. However, the system needs to rely on a trusted central server for global model aggregation. Besides, due to the potential misuse of spectrum by terrestrial users and malicious behaviors of the satellites in the FL, LEO satellite IoT is still facing system security and privacy preservation issues. The following threats are considered in the system.

1) *Privacy Leakage and Global Model Tamping*: A central server is vulnerable to attack and may collude with other parties.

2) *Malicious Terrestrial Users*: A malicious terrestrial user may increase the uplink transmit power for a better QoS after leasing the spectrum.

3) *Malicious Satellite Nodes*: A malicious satellite node may be fraudulent when transmitting the transaction data to the terrestrial server and may advertise fraudulent spectrum leasing services when they can not provide enough available spectrum.

In this paper, we propose a reputation-based blockchain combining FL to address the threats.

D. Problem Formulation

In LEO satellite IoT communication systems, satellites need to dynamically price spectrum based on the budgets of terrestrial users for spectrum resource leasing. This paper aims to maximize the benefits of LEO satellites while optimizing

spectrum resource management. The satellite benefit can be divided into two parts. The first part is the benefit obtained by leasing the idle spectrum which can be expressed as

$$u_t^{Spe,m} = p_t^m N_{pri,t}^m \quad (5)$$

where p_t^m denotes the spectrum pricing given by the satellite at time slot t , $N_{pri,t}^m$ denotes the number of users willing to lease this spectrum at the pricing p_t^m . The second part is the benefit obtained by contributing to the blockchain of the FL process which can be expressed as

$$u_t^{Rep,m} = \hat{p}_t^m N_{pow,t}^m \quad (6)$$

where \hat{p} denotes the reputation coefficient, l_t^m denotes the power control level of the satellite, and $N_{pow,t}^m$ denotes the number of users whose transmit power is lower than l_t^m . Thus, the problem can be formulated as follows

$$\begin{aligned} \max_{p,l} \quad & \sum_{m=1}^N (u_t^{Spe,m} + u_t^{Rep,m}) \\ \text{s.t.} \quad & a) \chi_a \in \{0, 1\}, \forall a \in \kappa \\ & b) 0 \leq p_t^m \leq p^{max} \\ & c) 0 \leq l_t^m \leq l^{max} \end{aligned} \quad (7)$$

where p^{max} , l^{max} denote the maximum price and power control level that can be set respectively. Constraint (7a) indicates that the number of spectrum accesses for any terrestrial user n is 0 or 1. Constraint(7b) and constraint(7c) ensure the spectrum pricing and power control level of the satellite are within maximum range, respectively.

IV. FRAMEWORK OF PRIVACY-AWARE SPECTRUM PRICING AND POWER CONTROL

In this paper, we propose a privacy-aware spectrum pricing and power control scheme to facilitate spectrum resource management in the LEO satellite IoT. The scheme can be divided into three phases namely spectrum leasing and local training phase, blockchain-driven federated aggregation phase and global model release phase. The whole process is presented in Sec. IV-A. The modelings of the utility function and reinforcement learning environment are introduced in Sec. IV-B and Sec. IV-C respectively. And we present the details of blockchain-driven federated aggregation in Sec. IV-D.

A. Whole Process

The whole process of the scheme and the proposed framework is as follows.

Spectrum Leasing and Local Training Phase: The operations in a local training round are presented in Fig. 3. Satellites are ready to lease their idle spectrum and set an initial price and initial uplink transmit power limit at first. Then, the satellite broadcasts the price and power control information to the terrestrial users (Label 1 in Fig. 3). After that, terrestrial users communicate with the satellites and decide to lease a certain spectrum (Label 2 in Fig. 3). After each round of trading, satellites transmit the collected trading information to their

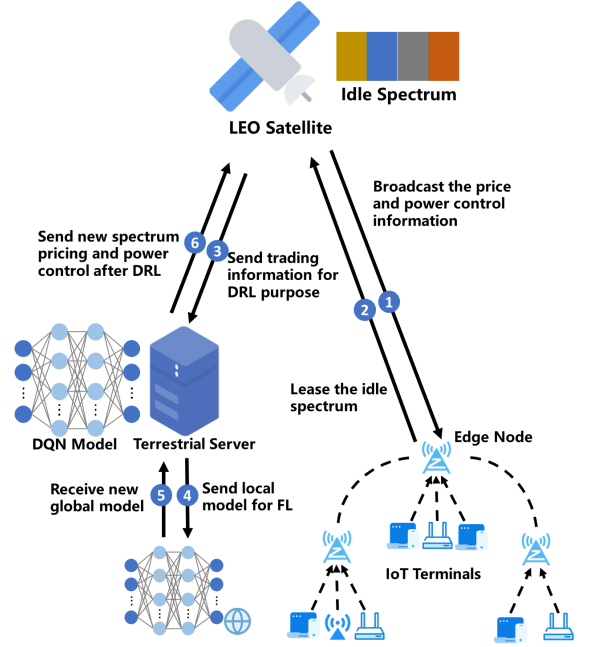


Fig. 3. Operations in a local training round.

terrestrial servers for local DRL (Label 3 in Fig. 3) and update their reputation records based on terrestrial users' behaviors. In addition, the servers record part of the trading information, verify the satellites' reputation records and send the local model to the Private Permissioned Blockchain network (Label 4 in Fig. 4) in preparation for the blockchain-driven federated aggregation in the next phase. After receiving the new global model (Label 5 in Fig. 3), servers transmit the new spectrum pricing and power control levels back to the satellite (Label 6 in Fig. 6).

Blockchain-driven Federated Aggregation Phase: After several rounds of local training, each terrestrial server broadcasts the trading record in the Private Permissioned Blockchain network. The server with the highest reputation record aggregates the global model and performs the records package and block generation for the federated aggregation round. Then, the server gets a reward for the contribution and puts its reputation record to 0.

Global Model Release Phase: The server broadcasts the global model and each server starts the next round of training based on the global model.

B. Modeling of Utility Function

Throughout the process of leasing spectrum between terrestrial users and LEO satellites, LEO satellites price their idle spectrum and terrestrial users select spectrum to lease according to their required QoS. Specifically, to maximize their benefits, LEO satellites need to set the appropriate price for the spectrum. Whether a terrestrial user chooses to lease a certain spectrum and the amount of the satellite's revenue after leasing depends on the user's budget for spectrum leasing,

m , u_t^m denotes the utility of satellite m , i_t^m denotes the average interference to terrestrial users after the last round of spectrum leasing and l_t^m denotes the power control level for the idle spectrum, respectively.

- **Action:** After obtaining the state, the satellite will choose an action a_t^m to change the spectrum pricing and the received power control level to find a higher utility. The action \mathcal{A}_t^m of the agent at time slot t can be described as

$$\mathcal{A}_t^m = [\delta_t^m, \rho_t^m] \quad (11)$$

where δ_t^m denotes the price level decision, ρ_t^m denotes the power control level decision, and $\delta_t^m \in \{0, 1\}$, $\rho_t^m \in \{0, 1\}$. 0 means decrease one level, 1 means increase one level.

- **Policy:** We define the policy $\pi(\mathcal{S}_{t+1}^m | \mathcal{S}_t^m, \mathcal{A}_t^m)$ to mapping from states to actions, which denote the probability that the agent m selects action \mathcal{A}_t^m from state \mathcal{S}_t^m into a new state \mathcal{S}_{t+1}^m at time slot t .
- **Reward:** To find an appropriate price and power control level to maximize the LEO satellites' utility, the reward will play a key role in evaluating the learning policy. The reward in this paper can be given as

$$\mathcal{R}_t^m = u_t^m - u_{t-1}^m \quad (12)$$

To maximize the long-term cumulative reward, the agent needs to search for an optimal policy $\pi(\mathcal{S}_{t+1}^m | \mathcal{S}_t^m, \mathcal{A}_t^m)$ when interacting with the environment. During the process, agents execute an action \mathcal{A}_t^m , transitioning from the current state \mathcal{S}_t^m to the next state \mathcal{S}_{t+1}^m . Specifically, each state transitioning of the agent is based on the transition probability. After each state transition, agents receive a reward \mathcal{R}_t^m from the environment. The long-term accumulation reward is called the state-value function which is defined as

$$V^\pi(\mathcal{S}) = \mathbb{E}_\pi \left[\sum_{t=1}^{\infty} \gamma_t \mathcal{R}_t^m(\mathcal{S}_{t+1}^m, \mathcal{A}_t^m) | \mathcal{S}_{t+1}^m = \mathcal{S} \right] \quad (13)$$

Since the reward obtained after each interaction with the environment is immediate feedback, each decision is likely to have an impact on all subsequent states. Thus $\gamma_t^m \in (0, 1]$ is a discount factor indicating the proportion of the future rewards' value of the current moment. And the optimal state-value function $V^*(\mathcal{S})$ is defined as

$$V^*(\mathcal{S}) = \max_{\pi} V^\pi(\mathcal{S}) \quad (14)$$

In this paper, DDQN is introduced to address the MDP problems which can adapt to the environment with uncertainty. And the long-term accumulative reward is expressed by the Q-value function. Each agent has two neural networks which are basic network \mathcal{B} and target network \mathcal{T} . The basic network \mathcal{B} of each agent is updated in real-time while the target network \mathcal{T} is updated based on the updating frequency factor f to avoid overestimating the Q-value. The Q-value function can be given by

$$Q^\pi(\mathcal{S}, \mathcal{A}) = \mathbb{E}_\pi \left[\sum_{t=1}^{\infty} \gamma_t \mathcal{R}_t^m(\mathcal{S}_t^m, \mathcal{A}_t^m) | \mathcal{S}_t = \mathcal{S}, \mathcal{A}_t^m = \mathcal{A} \right] \quad (15)$$

So the optimal Q-function is defined as

$$Q^*(\mathcal{S}, \mathcal{A}) = \max_{\pi} Q^\pi(\mathcal{S}, \mathcal{A}) \quad (16)$$

And based on the Bellman Optimality Equation, the Q-value function can be defined as

$$Q(\mathcal{S}_t^m, \mathcal{A}_t^m) = \mathcal{R}_t^m + \gamma_t Q(\mathcal{S}_{t+1}^m, \operatorname{argmax}_{\mathcal{A}_t^m \in \mathcal{A}} Q(\mathcal{S}_{t+1}^m, \mathcal{A}_t^m; \mathcal{B}_t^m); \mathcal{T}_t^m) \quad (17)$$

Then the Q-value function is updated by

$$Q_{t+1}(\mathcal{S}_t^m, \mathcal{A}_t^m) = (1-l)Q_t(\mathcal{S}_t^m, \mathcal{A}_t^m) + l(\mathcal{R}_t^m + \gamma_t Q(\mathcal{S}_{t+1}^m, \operatorname{argmax}_{\mathcal{A}_t^m \in \mathcal{A}} Q(\mathcal{S}_{t+1}^m, \mathcal{A}_t^m; \mathcal{B}_t^m); \mathcal{T}_t^m)) \quad (18)$$

where $l \in (0, 1]$ denotes the learning rate.

The user selects an action to execute based on ϵ -policy in each training step, which can be expressed as

$$\mathcal{A}_{t+1}^m = \begin{cases} \mathcal{A}_{random} & P = \epsilon \\ \operatorname{argmax}_{\mathcal{A}_{t+1}^m \in \mathcal{A}} Q(\mathcal{S}_{t+1}^m, \mathcal{A}_{t+1}^m) & P = 1 - \epsilon \end{cases} \quad (19)$$

The details and the whole process of the local DDQN model training are presented in Fig. 4 and Algorithm 1. Each LEO satellite acts as an agent and first initializes its basic network parameter w and target network parameter \hat{w} (Line 2-3 in Algorithm 1). And they perform E episodes in each local training round. When performing local DDQN, the LEO satellite first observes the current state \mathcal{S}_t^m which is the current spectrum leasing and power control conditions (Label 1 in Fig. 4, Line 10), and selects an action \mathcal{A}_t^m based on the target network and the policy π (Label 2, Line 11). The agent randomly selects an action from action space \mathcal{A} with probability ϵ and selects the action with maximum Q-value with probability $1 - \epsilon$. After executing the action \mathcal{A}_t^m , an immediate reward \mathcal{R}_t^m and a new state \mathcal{S}_{t+1}^m are obtained (Label 3, Line 13) which construct the experience together with the action \mathcal{A}_t^m and state \mathcal{S}_t^m . Then the experience of that episode is stored in the memory buffer (Label 4, line 14). Next, a batch is randomly drawn from the memory buffer for updating the basic network (Labels 5-6, Line 15). The target network will be updated for every f local training round.

D. Blockchain-driven Federated Aggregation

When satellites lease their idle spectrum to terrestrial users, the security of some users' information and satellites' information could be an important issue. To improve the model training efficiency while protecting sensitive information, FL is introduced to the satellite IoT in this paper. In the satellite IoT, the data owned by individual devices is limited due to the coverage area and time, and these data can not be shared among devices to better improve the efficiency of dynamic spectrum pricing and trading because of the sensitivity of the transaction information involved. Instead of obtaining the original sensitive data, FL aggregates the local training model parameters of each user to form a global model and sends it to each user, which is an effective improvement in the related issue. However, in traditional FL, centralized global model aggregation remains a threat to the privacy-preserving of local devices. If the server aggregating the global model is

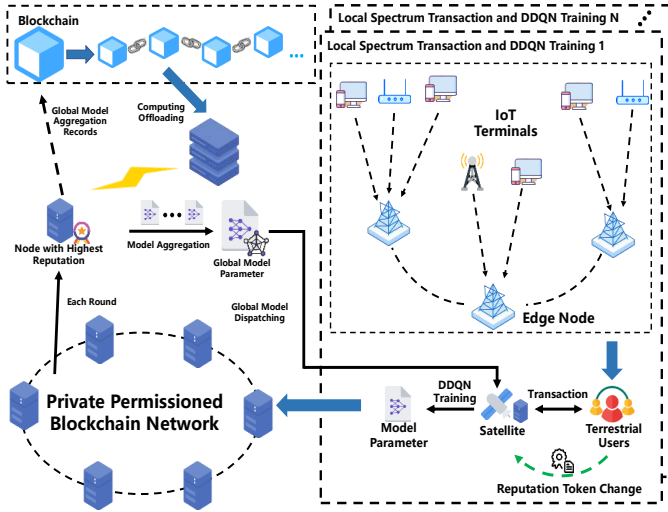


Fig. 5. Framework of Reputation-based Blockchain Network and FL Process

malicious or the server is attacked, the spectrum pricing and spectrum trading of the whole IoT system will be paralyzed. Thus, based on the feature of LEO satellite IoT communicating and transacting with terrestrial users, this paper proposes a reputation-based blockchain to provide decentralized global model aggregation and permission for users to join the IoT, instead of using a vulnerable central server.

As shown in Fig. 5, the network of Reputation-based Blockchain involves several components.

- **Satellite:** Satellite provides the idle spectrum to terrestrial users and trains the local DDQN model to search the optimal spectrum price and power control.
- **Terrestrial users:** Terrestrial users are the spectrum demanders. They decide whether to lease the idle spectrum provided by a certain satellite based on their budget and requirements for spectrum quality.
- **Reputation token:** Each satellite that is a member of a private permissioned blockchain network has a reputation token record. The reputation token record of each satellite changes for each round of dynamic spectrum access by terrestrial users. If there are no users with malicious behavior in this access round, the number of reputation tokens for that satellite is the original number of reputation tokens plus the newly acquired reputation tokens. Instead, if there is a malicious user in this access round, the number of reputation tokens for the satellite is the original number of reputation tokens minus the penalty incurred for the malicious user. The reputation record of a satellite can be expressed as

$$Rep_t^m = \begin{cases} Rep_{t-1}^m + \mathcal{V}_t^{acc} & \text{no malicious users} \\ Rep_{t-1}^m - \mathcal{V}_t^{mal} & \text{malicious users appear} \end{cases} \quad (20)$$

where Rep_t^m denotes the reputation token, \mathcal{V}_t^{acc} denotes the newly acquired reputation token based on the situation that no malicious users appear and \mathcal{V}_t^{mal} denotes the newly lost reputation token based on the situation that

Algorithm 2 Process of Global Model Aggregation and Blockchain Updating

- 1: **Initialization:**
- 2: Model Aggregation frequency f'
- 3: **for** each global training round **do**
- 4: Each node updates the reputation Rep_t^m based on the reputation mechanism.
- 5: **if** global training round mod $f' == 0$ **then**
- 6: Each node broadcasts the model parameter to each of the other nodes of the private permissioned blockchain network.
- 7: Get the list by ranking the reputation of each node from highest to lowest.
- 8: **for** each node of the list **do**
- 9: **if** node is online **then**
- 10: The node aggregates the global model and generates the block.
- 11: The node sends the model to other nodes who locally train the model.
- 12: The node receives the reward for model aggregation and block generation.
- 13: End this round of global training.
- 14: **else if** node is offline **then**
- 15: Select the next node.
- 16: **end if**
- 17: **end for**
- 18: **end if**
- 19: **end for**

malicious users appear respectively. Then \mathcal{V}_t^{acc} and \mathcal{V}_t^{mal} can be expressed as

$$\mathcal{V}_t^{acc} = \hat{p} l_t^m N_{pow,t}^{acc} \quad (21)$$

$$\mathcal{V}_t^{mal} = \hat{p} l_t^m N_{pow,t}^{mal} \quad (22)$$

where \hat{p} denotes the reputation coefficient, l_t^m denotes the power control level of the satellite, $N_{pow,t}^{acc}$ denotes the number of normal users whose transmit power is lower than l_t^m , $N_{pow,t}^{mal}$ denotes the number of malicious users. The malicious behavior of ground users is as follows. 1) The number of terrestrial users accessing the spectrum exceeds the limit. 2) Terrestrial users accessing the satellite's spectrum without meeting the required power level. 3) Terrestrial users access the spectrum for too long or too short a period of time based on the spectrum lease contract.

- **Edge node:** Edge node is responsible for verifying transaction users, conducting spectrum transactions and saving transaction records. Each terrestrial user pays money to the satellite through the edge node.

Algorithm 2 shows the process of global model aggregation and blockchain updating. Model aggregation frequency f' is initialized first. After each round of spectrum transactions between satellites and the covered area's terrestrial users, each satellite node in the private permissioned blockchain network updates its reputation record based on the behaviors. When the global training round mod f' equals 0, it is the

TABLE II
PARAMETER SETTINGS

Parameter	Value
Learning rate l	0.001
Number of devices	4
Probability ϵ	0.2
Batch size	16
Number of terrestrial users	1000
Budget scale of terrestrial user	30
Discount factor γ	0.95
Reputation coefficient \hat{p}	1

round for global aggregation and updating. Each satellite node broadcasts its local parameter to each of the other satellite nodes of the blockchain network. And then rank each satellite's reputation from highest to lowest. The aggregation priority of each satellite node is represented in list order. If the node is online, then it becomes the aggregation node in this round. And if the node is offline, the next node will be considered. For the aggregation node, once the node is confirmed, it first aggregates the global model and generates the block. And then the node sends the model to other nodes who locally train the model. After that, the node will receive the reward for the contribution.

E. Complexity Analysis

Let \mathcal{N} , \mathcal{L}_i define the training layer and the number of the neurons in the i -th layer. Thus, computational complexity in each training time step for each agent is $O(\sum_{i=0}^{\mathcal{N}} \mathcal{L}_i \mathcal{L}_{i+1})$. And let \mathcal{M} , \mathcal{K} and \mathcal{E} denote the number of the trained models, total training round and episodes in each training round, respectively. The computational complexity can be expressed by $O(\mathcal{M}\mathcal{K}\mathcal{E} \sum_{i=0}^{\mathcal{N}} \mathcal{L}_i \mathcal{L}_{i+1})$ [38]–[40]. The high computational complexity of the local training phase can be performed offline for a finite number of episodes on terrestrial servers.

For the FL phase, let $\mathcal{D}(t)$ denote the number of devices involved at time slot t . Hence, the computational complexity is $O(1/\sqrt{\sum_{t=1}^{T^{FL}} \mathcal{D}(t)})$.

V. NUMERICAL RESULTS

In this section, simulations are conducted to present the performance of the scheme.

A. Simulation Settings

We generated 1000 terrestrial users who were interested in purchasing the LEO satellite spectrum. Each user randomly generated its own spectrum trading budget within the budget scale and access power requirements. Each LEO satellite runs a DRL agent with a two-layer neural network locally. Besides, we set the learning rate l as 0.001, number of LEO satellite DRL agents as 4, probability ϵ as 0.2, batch size as 16, number of terrestrial users as 1000, budget scale of terrestrial user as 30 and discount factor γ as 0.95. The parameter is shown in TABLE I.

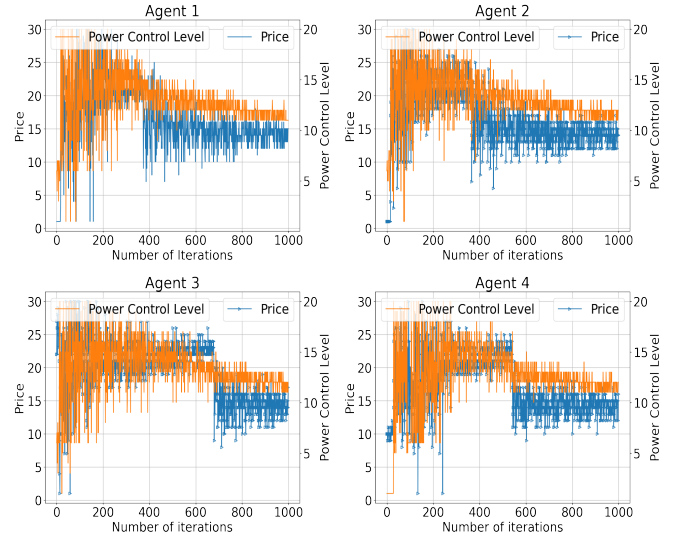


Fig. 6. Pricing and power control performances of the four agents

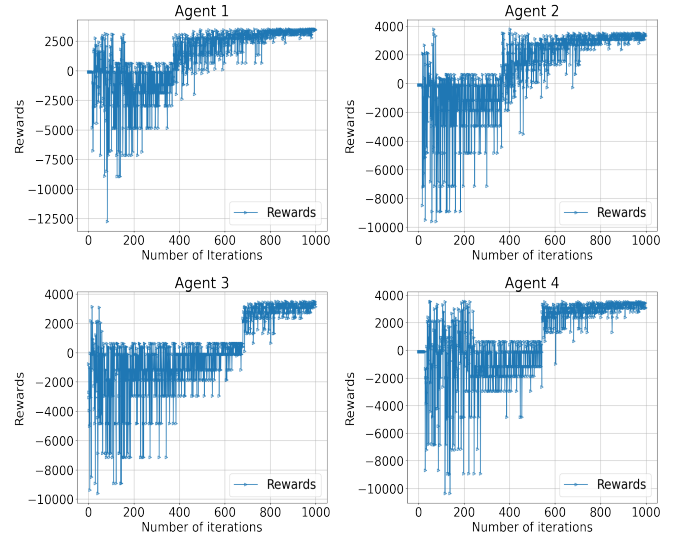


Fig. 7. Rewards performances of the four agents

B. Case Study

In Fig. 6, Fig. 7 and Fig. 8, we simulated the pricing and power control for 4 agents in 1000 iterations. In this simulation, the global model aggregation algorithm is FedAvg. Fig. 5 shows the pricing and power control. Fig. 6 and Fig. 7 show the Rewards and Utility of the satellite. We can see that in the first iterations, the power control and pricing of the 4 agents are in the process of oscillation. At about 400 iterations, agent 1 and agent 2 first start to converge. Then, agent 3 and agent 4 start to converge after about 550 and 700 iterations, respectively. After about 800 iterations, all 4 agents can find the optimal pricing and power control scheme for the current situation. Note that the performance of agent 3 and agent 4 suddenly improves during the iterations. This is due to the collaborative training of these agents. Specifically, During

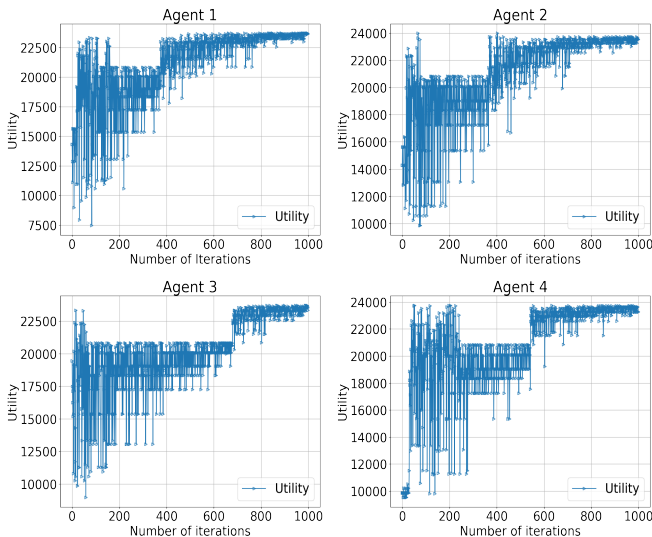


Fig. 8. Utility performances of the four agents

the training process, some agents may have learned positive actions while some have not yet. In this case, FL improves the efficiency of IoT nodes' local training.

In Fig. 9, we compared the performances of four agents in the FedAvg algorithm [41] and FedProx algorithm [42] in cases of no devices, one device, two devices and three devices which lead to different visibility. Particularly, the red line indicates the case that the visibility of the four agents is always maintained at 100 percent, which is regarded as the baseline. The blue line illustrates the case that the visibility of one agent, two agents and three agents is maintained at 80 percent in Fig. 8(a), Fig. 8(b) and Fig. 8(c), respectively. And the yellow line shows the case that the visibility of one agent, two agents and three agents is maintained at 60 percent in Fig. 8(a), Fig. 8(b) and Fig. 8(c). The details of the algorithms are given below.

- **FedAvg:** The global server initializes the global parameters, executes several rounds, and selects clients for training in each round. Next, each selected client simultaneously trains its own model with its own data locally based on the model from the global server, and uploads it back to the server afterwards. The global server aggregates the global models by averaging the parameters from each client to obtain the model for the next training round.
- **FedProx:** Based on the FedAvg algorithm loss function, a proximal term is introduced in the FedProx algorithm which makes the model parameters obtained by the client after local training not deviate too much from the initial server parameters.

As the baseline, the accuracy reaches around 81.8% in FedAvg and around 82.5% in FedProx after 300 rounds of training. In Fig. 8(a), the accuracy decreases with the visibility of the device and reaches approximately 78.6% in FedAvg and 79.2% when only one device has only 80% visibility. And when only one device has 60% visibility, the accuracy is approximately

73.9% in FedAvg and 74.8% in FedProx. This is because the satellite can not efficiently gather spectrum utilization information and lease requests from all terrestrial users when there are limitations in the visibility of the satellite. The data used for local training of the model deviates from the real data which also affects the global model. Comparing Fig. 8(a), Fig. 8(b) and Fig. 8(c), We can see that accuracy decreases with the number of devices with visibility limitations increases. The lowest case is when all three devices have 60% visibility, the accuracy is about 65.5% in FedAvg and about 69.5% in FedProx. This is due to the fact that as the number of devices with visibility limitations increases, the global model becomes more influenced by the local model of these devices. Besides, we can see the FedProx algorithm performs better than the FedAvg algorithm. It is noted that in the case of multiple devices where visibility limitations exist and the visibility is low, the accuracy improvement is greater in the FedProx. This is because the FedProx algorithm restricts the local model from deviating too far from the global model.

In Fig. 10, we compared the pricing and power control accuracy of the proposed scheme for different replay sizes which are 20, 60, 100 and 200 respectively. We set the training round as 400, and each training round has 60 steps. We can see that the accuracy for the replay size of 60, 100 and 200 improves about the same speed and is faster compared to the 20 replay size. Starting at around 55 rounds, the convergence rate gradually starts to slow down and converges at around 300 rounds. Note that finally when the replay size is 200, 100, and 60, the accuracy achieved is about 88%, 85%, and 81%, respectively. This is because the replay size has an impact on the effectiveness of model training. Specifically, a sufficiently large replay size ensures that the agent learns decisions that help the model improve its performance in a single training round. Hence, within a certain range, the larger the replay size is, the more efficient the agent learns. For the replay size of 20, it is only around the 200th training round that convergence begins. However, since the learning rate is dynamically decreasing, the final accuracy that can be achieved is only around 46%. The reason is the replay size is too small which will result in the difficulty of learning effective strategies during each round of training.

VI. CONCLUSION

In this paper, we consider the effective spectrum pricing and uplink transmit power control scheme for LEO satellite IoT. We first formulate a reinforcement problem based on the satellite communications features to maximize the benefits of leasing spectrum and power control. Next, a locally trained DRL-based scheme is proposed for satellites to find the optimal policy. Then, we further introduce a blockchain-driven FL framework to enhance the training collaboration while keeping the system distributed throughout the whole process to guarantee the security of local private information. We also conduct simulations to present the pricing and power control performances of agents that participate in the FL and compare the performance of the learning-based scheme and the non-learning-based scheme. Numerical results show the

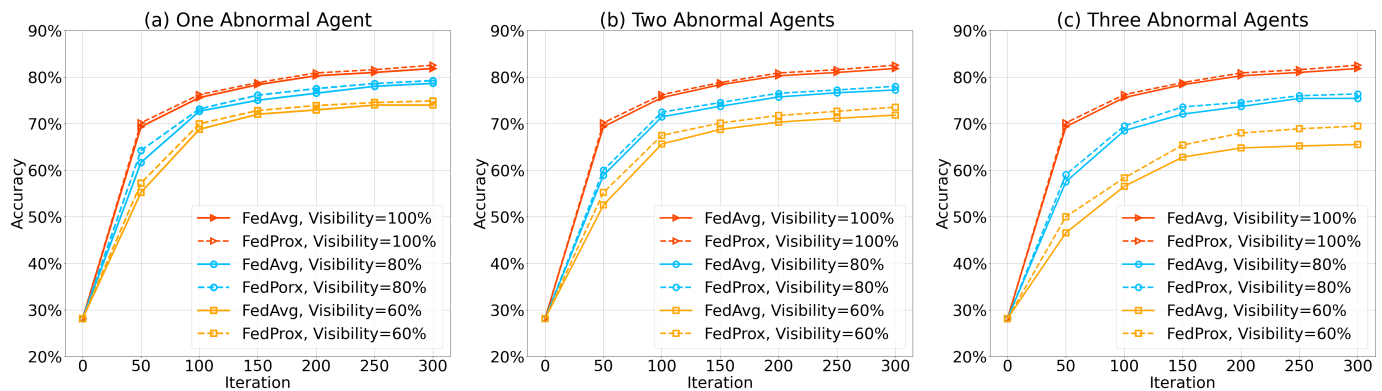


Fig. 9. Accuracy in FedAvg and FedProx in cases of no devices, one device, two devices and three devices which lead to different visibility

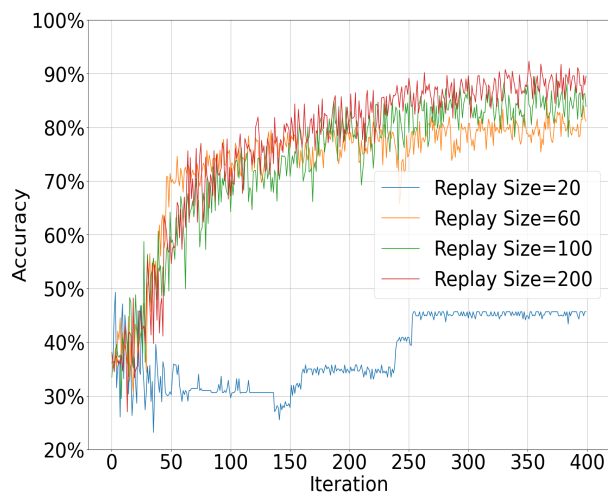


Fig. 10. Accuracy in different replay size

efficiency of the spectrum pricing and power control strategy proposed in this paper. In the process of LEO satellite idle spectrum leasing, terrestrial users may move to another area while still leasing the previous spectrum or there may be a sudden surge or decrease of users in that area after leasing a certain spectrum. In this case, such problems may arise: 1) The QoS obtained by the LEO satellite at this time may vary, such as changes in interference and power attenuation due to different numbers of accesses and distance values. 2) The latest price of that spectrum may fluctuate. Therefore, in our future work, we will focus on the spectrum allocation in a receptive and timely manner while maintaining the pricing in an acceptable range.

REFERENCES

- [1] C. Ding, J.-B. Wang, M. Cheng, M. Lin, and J. Cheng, "Dynamic transmission and computation resource optimization for dense leo satellite assisted mobile-edge computing," *IEEE Trans. Commun.*, vol. 71, pp. 3087–3102, May 2023.
- [2] H. Yao, L. Wang, X. Wang, Z. Lu, and Y. Liu, "The space-terrestrial integrated network: An overview," *IEEE Commun. Mag.*, vol. 56, pp. 178–185, Sep. 2018.
- [3] D. S. Lakew, A.-T. Tran, A. Masood, N.-N. Dao, and S. Cho, "A review on satellite-terrestrial integrated wireless networks: Challenges and open research issues," in *Proc. Int. Conf. Inf. Netw. (ICOIN)*, pp. 638–641, Jan 2023.
- [4] J. Fomon, "Starlink slowed in q2, competitors mounting challenges." [Online]. Available: <https://www.ookla.com/articles/starlink-hughesnet-viasat-performance-q2-2022>.
- [5] FCC, "Kuiper systems, llc application for authority to deploy and operate a ka-band non-geostationary satellite orbit system," 2020. [Online]. Available: <https://www.fcc.gov/document/fcc-authorizes-kuiper-satellite-constellation>.
- [6] "Fcc authorizes boeing broadband satellite constellation," 2021. [Online]. Available: <https://www.fcc.gov/document/fcc-authorizes-boeing-broadband-satellite-constellation>.
- [7] X. Luo, H.-H. Chen, and Q. Guo, "Leo/vleo satellite communications in 6g and beyond networks – technologies, applications and challenges," *IEEE Network*, pp. 1–1, 2024.
- [8] K. S. Gill, P. Kryszkiewicz, P. Sroka, A. Kliks, and A. M. Wyglinski, "Memory enabled bumblebee-based dynamic spectrum access for platooning environments," *IEEE Trans. Veh. Technol.*, vol. 72, pp. 5612–5627, May 2023.
- [9] H.-H. Chang, Y. Song, T. T. Doan, and L. Liu, "Federated multi-agent deep reinforcement learning (fed-madrl) for dynamic spectrum access," *IEEE Trans. Wirel. Commun.*, pp. 1–1, 2023.
- [10] T. Safdar Malik, K. Razzaq Malik, A. Afzal, M. Ibrar, L. Wang, H. Song, and N. Shah, "RI-iot: Reinforcement learning-based routing approach for cognitive radio-enabled iot communications," *IEEE Internet Things J.*, vol. 10, pp. 1836–1847, Jan 2023.
- [11] A. S. Shafiq, B. Lorenzo, S. Glisic, and Y. Fang, "Optimization of 3d spectrum management in future wireless networks," *IEEE Trans. Veh. Technol.*, vol. 72, pp. 2407–2423, Feb 2023.
- [12] J. Huang, Y. Yang, L. Yin, D. He, and Q. Yan, "Deep reinforcement learning-based power allocation for rate-splitting multiple access in 6g leo satellite communication system," *IEEE Wireless Communications Letters*, vol. 11, no. 10, pp. 2185–2189, 2022.
- [13] J. Li, K. Xue, D. S. L. Wei, J. Liu, and Y. Zhang, "Energy efficiency and traffic offloading optimization in integrated satellite/terrestrial radio access networks," *IEEE Trans. Wirel. Commun.*, vol. 19, pp. 2367–2381, April 2020.
- [14] P. Gu, R. Li, C. Hua, and R. Tafazolli, "Dynamic cooperative spectrum sharing in a multi-beam leo-geo co-existing satellite system," *IEEE Transactions on Wireless Communications*, vol. 21, no. 2, pp. 1170–1182, 2022.
- [15] A. Kaur, J. Thakur, M. Thakur, K. Kumar, A. Prakash, and R. Tripathi, "Deep recurrent reinforcement learning-based distributed dynamic spectrum access in multichannel wireless networks with imperfect feedback," *IEEE Trans. Cogn. Commun. Netw.*, vol. 9, pp. 281–292, April 2023.
- [16] M. A. Qureshi, E. Lagunas, and G. Kaddoum, "Reinforcement learning for link adaptation and channel selection in leo satellite cognitive communications," *IEEE Communications Letters*, vol. 27, no. 3, pp. 951–955, 2023.
- [17] M. Yang, J. Chen, Z. Ding, Y. Liu, L. Lv, and L. Yang, "Joint power allocation and decoding order selection for noma systems: Outage-optimal strategies," *IEEE Transactions on Wireless Communications*, vol. 23, no. 1, pp. 290–304, 2024.
- [18] Z. Gao, A. Liu, and X. Liang, "The performance analysis of downlink

- noma in leo satellite communication system,” *IEEE Access*, vol. 8, pp. 93723–93732, 2020.
- [19] N. Torzkaban and M. A. Amir Khojastepour, “Shaping mmwave wireless channel via multi-beam design using reconfigurable intelligent surfaces,” in *2021 IEEE Globecom Workshops (GC Wkshps)*, pp. 1–6, 2021.
- [20] Q. Cong and W. Lang, “Deep multi-user reinforcement learning for centralized dynamic multichannel access,” in *Proc. Int. Conf. Intel. Comput. Signal Processing (ICSP)*, pp. 824–827, April 2021.
- [21] M. A. Yadav, Y. Li, G. Fang, and B. Shen, “Deep q-network based reinforcement learning for distributed dynamic spectrum access,” in *Proc. Int. Conf. Comp. Commun. Artif. Intel. (CCAI)*, pp. 1–6, May 2022.
- [22] Y. Huang, H. Cui, Y. Hou, C. Hao, W. Wang, Q. Zhu, J. Li, Q. Wu, and J. Wang, “Space-based electromagnetic spectrum sensing and situation awareness,” *Space: Science & Technology*, vol. 4, p. 0109, 2024.
- [23] C. Sun, X. Li, J. Wen, X. Wang, Z. Han, and V. C. M. Leung, “Federated deep reinforcement learning for recommendation-enabled edge caching in mobile edge-cloud computing networks,” *IEEE J. Sel. Areas Commun.*, vol. 41, pp. 690–705, March 2023.
- [24] S. Warnat-Herresthal, H. Schultze, K. L. Shastry, *et al.*, “Swarm learning for decentralized and confidential clinical machine learning,” *Nature*, vol. 594, pp. 265–270, May 2021.
- [25] J. Passerat-Palmbach, T. Farnan, M. McCoy, J. D. Harris, S. T. Manion, H. L. Flannery, and B. Gleim, “Blockchain-orchestrated machine learning for privacy preserving federated learning in electronic health data,” in *Proc. Int. Conf. Blockchain (Blockchain)*, pp. 550–555, Nov 2020.
- [26] Z. Li, W. Wang, Q. Wu, and X. Wang, “Multi-operator dynamic spectrum sharing for wireless communications: A consortium blockchain enabled framework,” *IEEE Trans. Cogn. Commun. Netw.*, vol. 9, pp. 3–15, Feb 2023.
- [27] L. Xie, S. Meng, W. Yao, and X. Zhang, “Differential pricing strategies for bandwidth allocation with lfa resilience: A stackelberg game approach,” *IEEE Transactions on Information Forensics and Security*, vol. 18, pp. 4899–4914, 2023.
- [28] A. Pourkabirian, M. H. Anisi, and F. Kooshki, “A game-based power optimization for 5g femtocell networks,” *Computer Communications*, vol. 177, pp. 230–238, July 2021.
- [29] S. Chan, H. Lee, S. Kim, and D. Oh, “Intelligent low complexity resource allocation method for integrated satellite-terrestrial systems,” *IEEE Wirel. Commun. Lett.*, vol. 11, pp. 1087–1091, May 2022.
- [30] Q. Tang, Z. Fei, and B. Li, “Distributed deep learning for cooperative computation offloading in low earth orbit satellite networks,” *China Commun.*, vol. 19, pp. 230–243, April 2022.
- [31] A. A. Hammadi, L. Bariah, S. Muhaidat, M. Al-Qutayri, P. C. Sofotasios, and M. Debbah, “Deep q-learning-based resource management in irl-assisted vlc systems,” *IEEE Transactions on Machine Learning in Communications and Networking*, vol. 2, pp. 34–48, 2024.
- [32] X. Liao, X. Hu, Z. Liu, S. Ma, L. Xu, X. Li, W. Wang, and F. M. Ghannouchi, “Distributed intelligence: A verification for multi-agent drl-based multibeam satellite resource allocation,” *IEEE Commun. Lett.*, vol. 24, pp. 2785–2789, Dec 2020.
- [33] Y. Liu, L. Jiang, Q. Qi, and S. Xie, “Energy-efficient space-air-ground integrated edge computing for internet of remote things: A federated drl approach,” *IEEE Internet Things J.*, vol. 10, pp. 4845–4856, March 2023.
- [34] H. Yang, J. Zhao, Z. Xiong, K.-Y. Lam, S. Sun, and L. Xiao, “Privacy-preserving federated learning for uav-enabled networks: Learning-based joint scheduling and resource management,” *IEEE J. Sel. Areas Commun.*, vol. 39, no. 10, pp. 3144–3159, 2021.
- [35] S. Yu, X. Chen, Z. Zhou, X. Gong, and D. Wu, “When deep reinforcement learning meets federated learning: Intelligent multimescale resource management for multiaccess edge computing in 5g ultradense network,” *IEEE Internet Things J.*, vol. 8, pp. 2238–2251, Feb 2021.
- [36] F. Li, K.-Y. Lam, J. Hua, K. Zhao, N. Zhao, and L. Wang, “Improving spectrum management for satellite communication systems with hunger marketing,” *IEEE Wireless Communications Letters*, vol. 8, no. 3, pp. 797–800, 2019.
- [37] F. Li, Z. Sheng, J. Hua, and L. Wang, “Preference-based spectrum pricing in dynamic spectrum access networks,” *IEEE Trans. Serv. Comput.*, vol. 11, pp. 922–935, Nov 2018.
- [38] C. Jiang and X. Zhu, “Reinforcement learning based capacity management in multi-layer satellite networks,” *IEEE Trans. Wirel. Commun.*, vol. 19, pp. 4685–4699, July 2020.
- [39] H. Yang, J. Zhao, K.-Y. Lam, Z. Xiong, Q. Wu, and L. Xiao, “Distributed deep reinforcement learning-based spectrum and power allocation for heterogeneous networks,” *IEEE Trans. Wirel. Commun.*, vol. 21, pp. 6935–6948, Sep 2022.
- [40] Z. Li, C. Jiang, and L. Kuang, “Double auction mechanism for resource allocation in satellite mec,” *IEEE Trans. Cogn. Commun. Netw.*, vol. 7, pp. 1112–1125, Dec 2021.
- [41] B. McMahan, E. Moore, D. Ramage, S. Hampson, and B. A. y. Arcas, “Communication-Efficient Learning of Deep Networks from Decentralized Data,” in *Proc. Int. Conf. Artif. Intel. Stats*, vol. 54, pp. 1273–1282, Apr 2017.
- [42] L. Tian, S. Anit, Kumar, Z. Manzil, S. Maziar, T. Ameet, and S. Virginia, “Federated optimization in heterogeneous networks,” *arXiv:1602.05629*, Jan 2023.